ANN Intelligent control based Wind-Solar PV-BES and DEGS Micro grid System for EV Charging Station

[1]K. Ravi Kiran, [2]K.Srinivasa Rao, [3]Ch.Ranga Raghava Reddy, [4]V.Ramani, [5]Mr. K Nagaraju
[1,2,3,4]B.Tech. Student, [5]Assistant Professor, EEE Department, Kallam Haranadhareddy Institute of Technology, Guntur (DT), Andhra Pradesh, India

Abstract — Demand for grid power or DG (Diesel Generator) to recharge electric cars is projected to rise. Solar PV arrays, BES, diesel generators, and grid-based EV charging stations enable on-demand charging (CS). Many innovative methods are being developed to reduce the grid effect of EV recharging. The charging station has a solar PV array and a BES. In the lack of solar PV array production, the charging station draws power from the grid or a diesel generator. To maximize fuel economy, DG electricity is always pulled at 80-85% loading. One of its key features is a wind-powered PMBLDC generator. Instead, we employ batteries and year-round wind power. Unreliable data transmitted between a vehicle and a grid or DG set If not controlled appropriately, these failures might cause unwanted plant outages. In EV grid and DG set integration, the vehicle to grid and DG set controller is critical. As a result, this study presents an ANN-based intelligent controller with data integrity and correction checks. As a result, the intelligent controller can reduce mistakes by selecting how much power to send to EVs. The PCC voltage is coordinated with the grid/generator voltage. Also, the charging station transfers electricity from automobile to grid, dwelling, and vehicle.

Keywords— EV Charging Station, Solar PV Generation, Power Quality, DG Set Wind uncertainty, High Wind penetration.

I. INTRODUCTION

A charging pattern that fulfils the requirements for competitive energy prices and load PAR is required for the incorporation of big electric cars (EVs) (peak to average ratio). The Indian region is accessible nearly all year. Unlike solar PV, wind and hydro energy are location specific. Wind energy is best used at the coast, whereas hydro energy is best used up north. The most urgent challenge is synchronising grid-connected EVs with intermittent renewable energy sources like wind and solar. Dumb Charging of Plug-In EVs may result in the grid charging several electric vehicles at the same time [2]. It assumes drivers would park their cars in convenient areas when not in use and will recharge them when their batteries run low. This may cause a load spike the grid cannot cope. Smart charging is a charging plan that adjusts the power consumption to the available power generation [3]. Renewable energy sources such as wind farms and photovoltaic (PVs) are extensively employed, and smart EV charging might be a key factor in increasing adoption [4]. Electric vehicles (EVs) and the grid must be connected via an intelligent controller in order to exchange power in a real-time application that has been evaluated by researchers. It is proposed in [5] to utilise the smart grid's potential for EVs by using intelligent fuzzy logic-based controllers, namely fuzzy load and fuzzy voltage. To propose an effective EV charging scheduling solution that considers the Greek interconnected power grid and future scenarios with high installed Wind Capacity. This study's new features include building a model for the uncertainty of wind power production and load demand using historical data, and implementing a smart charging scheduling technique using stochastic wind generation and demand data (Fig. 2). However, integrating renewable energy-based charging stations into current charging systems adds a power conversion step, increasing system complexity and power loss. A separate controller for each conversion step must also be attached to the current system. As a consequence, creating an integrated system with multifunctional and multimode capabilities is vital. The creation of a renewable energy charging station took a long time. Ugirumurera et al. [6] investigated the need for renewable energy in EV charging stations. Mouli et al.

 DOI : 10.35291/2454-9150.2022.0363

propose to use a high-power bidirectional EV charger, however this charger will not support AC charging. PV and electric vehicle (EV) charging may be combined with a three-port converter developed by Monterio et al. [7]. The intended charger, therefore, disregards the charger's current distortions. Singh et al. [8] developed a modified z-source converter for use in conjunction with a photovoltaic array/grid-connected EV charger. The charger, however, is not meant for island usage. As a consequence, it cannot allow EV charging without a grid. Using a hybrid optimization technique, Chaudhari et al. [9] suggest regulating battery storage to decrease charging station running costs while maximising solar PV production. Kineavy et al. [10] recommended employing on-site PV generated power in combination with an EV charging station to maximise solar PV array utilisation while decreasing grid influence. Zhang et al. [11] explored when to install a dual-mode EV charging station in the workplace. The PV array-powered charging station (CS) is also suitable for onsite location to maximise service quality and minimise charging grid influence [12]. Kandasamy et al. [13 studied a commercial building-based solar PV array system's loss of a storage battery. Wind energy-powered CS is helpful for EV since it is accessible day and night [14]-[15]. In recent years, EVs have been used as a distributed energy supply for a variety of applications. Reactive/active power filtering and vehicle-to-home applications can all benefit from a CS based on a PV array, according to Singh et al. EVs and residences can use a grid-connected PV array built by Saxena et al [17]. A multi-mode power management technique for a home PV-storage battery system was presented by Razmi et al. [18]. Kikusato et al. [20] and Erdinc, Hafiz, and colleagues (19) have all made significant contributions in this area. Research done on renewable energy charging stations optimises numerous aspects of charging, including the size of the renewable energy source, the size of the storage unit, and driving patterns. Only a few magazines, on the other hand, have actually constructed a charging station powered by renewable energy. In addition, the performance of charging stations in real-world circumstances is rarely assessed. In addition, the vast majority of studies focus on CS performance in grid-connected or isolated modes. Even if the sun is shining, the solar PV panel is inefficient because of its single mode of operation in grid-connected mode. A fluctuating sun's irradiance disrupts the PV system's output when it is in islanded mode. So a storage battery is required to counterbalance fluctuating solar irradiation. The maximum power point tracking (MPPT) feature must be turned off in order to prevent the storage battery from being overcharged[1]. In order to maximise the energy efficiency of PV arrays, this study proposes a control system (CS) that supports islanded, grid-connected, and DG set-connected PV arrays. There have been several articles [21] that have looked at both islanded and grid linked approaches. They are operated independently of one another, and there is no automated mode change. Without automatic mode change, PV array electricity and EV charging would be terminated. This research provides an automated mode switching logic that enables the controller to switch between several operating modes depending on PV array power and EV charging demands. Because the PV array is intermittent and unavailable at night, a storage battery is used alongside the PV array to keep the CS functioning. However, the storage battery's small storage capacity makes continuous backup problematic. Depleted energy storage and insufficient PV array power need grid support. Due to the scarcity of grid power, particularly in rural regions, the DG set may be necessary to keep the charge operating. The type of loading has an effect on the DG set's performance, which is not maximized. DG sets are frequently built for loads with a low harmonic component [22]. Due to the harmonic content of the EV current, EV charging has a major effect on the DG set's performance. Due to the harmonics and reactive current requirements of the EV charger, the DG set is constantly loaded to at least 80%. (VSC).

The following are the paper's significant contributions.

A PV array, energy storage, and DG set were used to build and experimentally evaluate a grid-integrated CS that allows EVs to be charged both DC and AC.

No hardware modifications are required to operate in island, grid-connected, and DG set connected modes using a single VSC and a single controller.

The development of a mode switching logic that enables the charging station to effortlessly switch modes in order to provide continuous charging.

Vehicle-to-vehicle and vehicle to grid power transfer (V2G) control strategy development for EV charging and grid assistance.

The active power filtering component of the charging station mitigates grid current harmonics, guaranteeing that the power exchange happens at unity power factor. This is required to ensure that the charging station adheres to the IEEE-519 standard.

An approach for managing the frequency and voltage of a DG set in the absence of a mechanical automatic voltage regulator.

Method for avoiding the storage battery from being overcharged by sending surplus power generated by the photovoltaic array back to the grid.

SYSTEM DESCRIPTION

 DOI : 10.35291/2454-9150.2022.0363

As shown in Fig. 1, a solar PV array, a storage battery, a DG set, and grid energy are utilized to charge the EV and provide the load tied to the charging station. The voltage source converter (VSC) has a DC link to which the solar PV array is connected through a boost converter, and the storage battery is connected directly to the DC connection. An sinusoidal currents. An excitation capacitor is connected to the SEIG's auxiliary winding. The main winding of the SEIG is also home to a teeny-tiny capacitance capacitor. A synchronizing switch is used between the PCC and the grid/DG set to manage the connection and disconnection of the charging station to the grid/DG set.

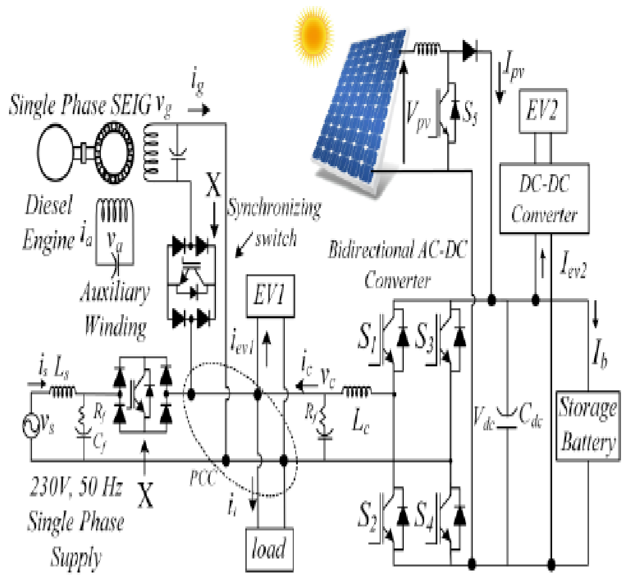

Fig. 1 Topology of charging station

CONTROL STRATEGIES

Various CS control techniques are explored in this article.

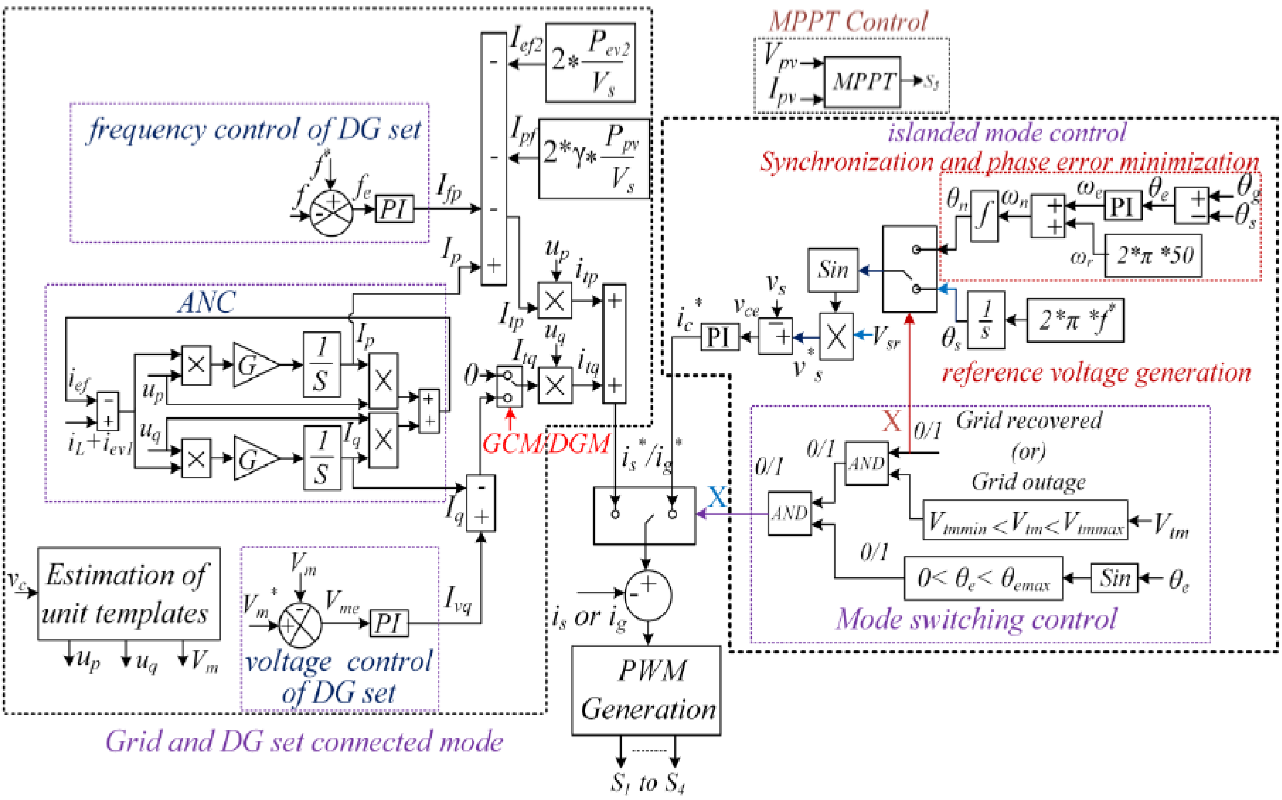

Fig. 2 Control of VSC in Islanded Mode and DG Set or Grid Connected Mode

 DOI : 10.35291/2454-9150.2022.0363

A. Control of VSC in Islanded Mode (Absence of DG Set and Grid

The CS's islanded control enables it to operate continuously in the absence of the grid, ensuring that the EV's AC and DC charging, as well as solar power generation, remain unaffected. The storage battery can handle DC charging and solar PV generating without requiring significant management changes. A separate controller for VSC must be used since there is no voltage reference when there is no grid; hence AC charging is not possible without it. With the circuitry shown in Figure 2, the island controller generates an internal voltage reference of 220V at 50 Hz using the frequency integration circuitry shown in Figure 2. The reference converter current is calculated by comparing the resultant reference to the converter's terminal voltage after voltage error is minimized with a proportional integral (PI) controller. The error minimization and production of reference currents are represented as,

$$i_c^*(s) = \overset{*}{i}_c(s-1) + z_{pv}\{v_{ce}(s) - v_{ce}(s-1)\} + z_{iv}v_{ce}(s) \quad (1)$$

When the reference current is compared to the measured converter current, a hysteresis controller is used to create the converter gate signals

Define abbreviations and acronyms the first time they are used in the text, even after they have been defined in the abstract. Abbreviations such as IEEE, SI, MKS, CGS, sc, dc, and rms do not have to be defined. Do not use abbreviations in the title or heads unless they are unavoidable.

Control of VSC in DG Set or Grid Connected Mode

The controller's job in grid linked mode is to select how much electricity to send to the grid. The DG set runs in constant power mode in connected mode to achieve optimum fuel economy. All situations need the controller to adjust for the EVs' harmonic and reactive current demands, which is done by computing the grid's reference current or the DG set from the EV current. It is used only in grid connected settings to estimate the EV's reference current. Reactive current and active current are both used to compute the DG set current in DG set connected mode. For the purpose of this investigation, the fundamental frequency current of the EV was extracted using an adaptive notch cancellation (ANC)[20]. The active and reactive currents are determined by the fundamental current at every zero crossing of the quadrature and in-phase unit templates, respectively, using the sample and hold logic. In grid linked mode, the total active and reactive currents are now as follows:

$$I_{sp} = I_p - I_{ef2} - I_{pf} \quad (2)$$

$$I_{sq} = 0$$

In grid-connected mode, only the active current of the EV is considered, while the reactive current is set to zero. On the other hand, the DG set linked mode utilises both the active and reactive current components of the EV. The total active and reactive current in the DG set connected mode is now as follows:

$$I_{sp} = I_p - I_{ef2} - I_{fp} - I_{pf} \quad (3)$$

$$I_{sq} = I_{vq} - I_q$$

Where Ief2 and Ipf denote the feed-forward terms of the EV2 and the photovoltaic array, respectively, and Ip and Iq denote the active and reactive currents of EV. The frequency and voltage regulators are referred to as Ifp and Ivq in the DG set connected mode. Ief2 is responsible for the vehicle-to-grid power transfer of the EV. In grid-connected mode, Ipf is the feed-forward term for the photovoltaic array that prevents the storage battery from being overcharged. Because the energy storage is directly attached to the DC connector, it cannot be charged in CC/CV mode. However, it is possible to guarantee that the storage battery is not overcharged under any circumstances. To prevent overcharging of a battery that is connected to the grid, solar PV generated power is sent into the grid. This is accomplished by including the grid-connected mode control's feed-forward term for the solar PV array, as illustrated in Fig. 2. In addition to the feed-forward term, a variable gain γ determines the percentage of PV array power delivered into the grid. According to the SOC information of the storage battery, the value of the constant γ is between 0 and 1. This means the γ" takes on the value of '1" when the storage battery is completely charged. However, if the storage battery is completely exhausted, the 'γ' becomes '0'. Finally, the grid or DG set's estimated reference current is as follows:

$$\overset{*}{i}_s \ or \ \overset{*}{i}_g = I_{tp} \times u_p + I_{tq} \times u_q \quad (4)$$

The DG set or grid voltage synchronization signals are up and qp, respectively (vg or vs). The switching signals are created utilizing a hysteresis controller and the detected and reference currents of the grid/DG set, as illustrated in Fig. 2.

DG Set Control for Voltage and Frequency

The DG set's frequency and voltage are regulated by decoupled control of the VSC, which operates the DG set at a single point. In decoupled control, active power controls the frequency, while reactive power controls the voltage. Two PI controllers are used to regulate the voltage and frequency. The PI control is as follows in terms of voltage regulation:

$$I_{vq}(s) = I_{vq}(s-1) + z_{vp}\{V_{me}(s) - V_{me}(s-1)\} + z_{vi}V_{me}(s) \quad (5)$$

Where Vme=Vm*-Vm and the zvi and zvp are the PI controller gains. Similarly, the frequency PI controller's discrete expression is as follows:

 DOI : 10.35291/2454-9150.2022.0363

$$I_{fp}(s)=I_{fp}(s-1)+z_{fp}\{f_e(s-1)\}+z_{fi}f_e(s) \qquad (6)$$

The fe and zkfp and zfi abbreviations stand for frequency error and PI gain, respectively. As shown in Figure 2, the frequency and voltage controllers' outputs are integrated in grid linked control. Grid-connected controllers' outputs drop to zero because the voltage and frequency are still being regulated by the grid.

B. Control of EV2

Constant current/constant voltage (CC/CV) is used to power an electric vehicle connected to a DC supply through a DC-DC converter. The EV charges in CC mode until the EV battery's terminal voltage reaches the voltage equal to full charge. After obtaining nearly the required terminal voltage in the near-full charge condition, the charging of the EVs is switched to CV mode. As demonstrated in Fig. 3, two PI controllers regulate the CC/CV charging mode. The current control stage's reference current is drawn from the external voltage loop.

$$\overset{*}{I}_{ev2}(s)=\overset{*}{I}_{ev2}(s-1)+Z_{evp}\{V_{er}(s-1)\}+z_{evi}V_{er}(s) \qquad (7)$$

Ver represents the error in the EV battery voltage, while zevp and zevi represent the controller gains.

The converter's switching signals are computed using the reference and measured battery currents through the use of the PI controller and PWM generator. For duty cycle computation, the PI controller is written as,

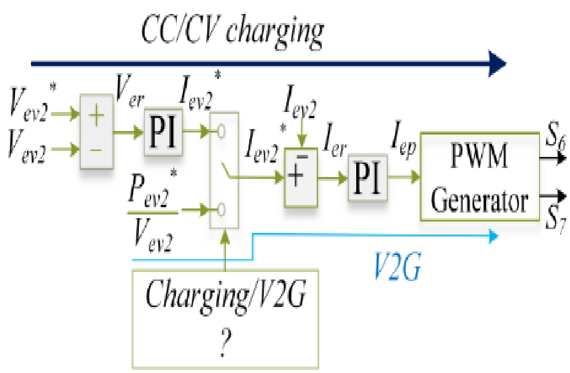

Fig. 3 EV2 control for CC/CV charging and V2G power transfer

C. The estimated reference charging current is as follows:

$$d_{ev}(s)=d_{ev}(s-1)+z_{ep}\{I_{er}(s)-I_{er}(s-1)\}+z_{ei}I_{er}(s) \qquad (8)$$

The battery current error is Ier, and the controller gains are zep and zei. The EV2 battery is depleted on the basis of the reference power for the V2G power transfer, and the controller follows the other route as illustrated in Fig. 3. The EV2 feed-forward term in Fig. 3 is controlled by the reference power.

Synchronization and Switching Control Because the charging station runs in a variety of modes depending on the generation and charging demand Mode switching strategies must be devised in such a way that the transition between modes is smooth and charging continues uninterrupted. The logic for mode transition is designed for scenarios such as islanded to grid connected and islanded to DG set connected modes. The phase difference between the two voltages is calculated first, and then the controller brings them into phase for synchronization. The PI controller adjusts the frequency of the voltage generated by the VSC in an islanded state using the logic represented in Figure 2. The phase minimization PI controller is written as,

$$\Delta\omega(s)=\Delta\omega(s-1)+z_{pa}\{\Delta\theta(s)-\Delta\theta(s-1)\}+z_{ia}\Delta\theta(s) \qquad (9)$$

Where zpa and zia are controller tuning parameters, and is phase difference.

The circumstances under which the CS functions in islanded mode are also shown in Fig. 2, as well as the criteria under which the mode shift must be performed. Once all of the synchronization requirements are satisfied, the control logic generates the enabling signal X='1' for the synchronizing switch.

IV. PRPOSED CONTROL TECHNIQUE

A. DEVELOPMENT OF THE WIND GENERATION CONCEPT

This section addresses an integrated wind energy generation process based on the platform, which includes a squirrel cage induction generator and a BEV operating in V2G mode. The use of wind energy, its conversion to electrical energy, and the connecting of the BEV's output to the distribution system via the V2G operating mode are depicted in Figure 1

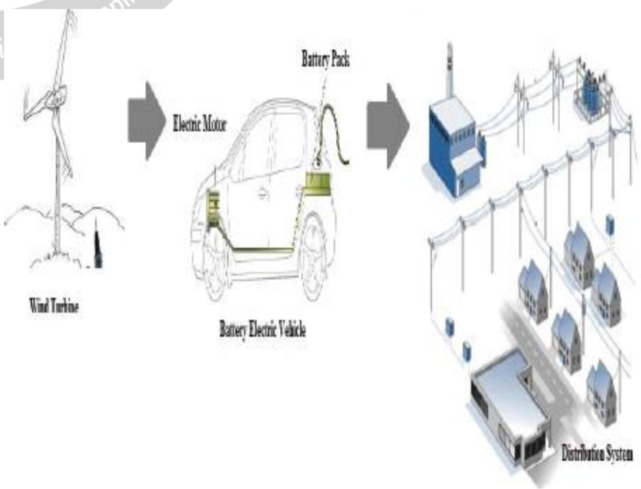

Fig. 4 Layout of the Integrated Project for Voltage Sag Mitigation

B. Wind Power Generation

The amount of energy generated by the wind is related to the cube of the wind speed. Drive train sensors and Mark Vle turbine controllers are employed in this research for

 DOI : 10.35291/2454-9150.2022.0363

superior load management performance in the class IIs wind domain, as shown in fig 1 and table 1.

Table 1: Specification of a Wind turbine

Class :	IEC IIs
Hub Heights :	80 meter
Tip Height :	123.5 meter
Noise :	107 dBA
Frequency :	50 Hz or 60 Hz
Blades :	42 meter
Technology :	Model based controls

Therefore, wind power generated:

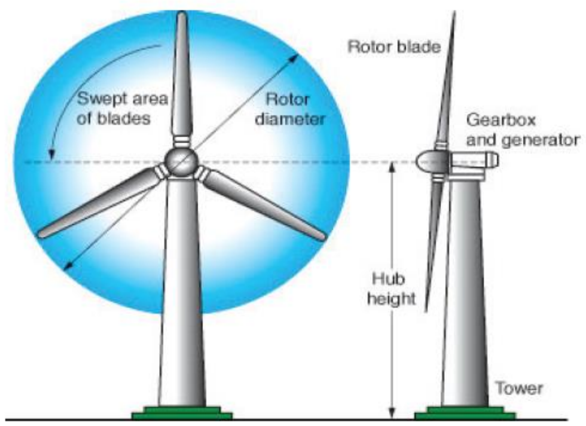

Fig. 5 Descriptive model of Wind Turbine

It is the air flow rate that enters and exits the turbine that determines the quantity of useable wind energy. The rotor blades' swept region is where the average speed passes. As a result, the mass flow rate of wind is:

$$P_m = \rho A \frac{V_1 + V_2}{2} \qquad (1)$$

$$P_m = \frac{1}{2}(V_1^2 - V_2^2)\frac{dm}{dt} \quad \text{w/m}^2 \qquad (2)$$

Combining eq (5) and (6)

$$P_m = \frac{1}{2}\rho A(V_1^2 - V_2^2)(V_1 + V_2) \qquad (3)$$

$$P_m = \frac{1}{4}\rho A V_1^3\left(1 - \frac{V_2^2}{V_1^2}\right)\left(1 + \frac{V_2}{V_1}\right) \qquad (4)$$

$$P_m = \frac{1}{2}\rho C_P A V_1^3 \qquad (5)$$

$$P_m = \frac{1}{2}\rho C_P A V_1^3$$

$$C_P = \left(1 - \frac{V_2^2}{V_1^2}\right)\left(1 + \frac{V_2}{V_1}\right)$$

Average speed of wind (w/s): $V_{av} = \frac{1}{n}\sum_{i=1}^{n} V_i$

Root mean cubic speed (w/s): $V_{rmc} = \sqrt[3]{\frac{1}{n}\sum_{i=n}^{n} V^3{}_i}$

Cubic power density (w/m2): $P_{rmc} = \frac{1}{2n}\sum_{i=n}^{n} \rho_i V^3{}_i$

Cubic energy density (wh/m2/yr)

$$E_{yw} = \frac{8760}{2n}\sum_{i=n}^{n} \rho_i V^3{}_i = 8760.\frac{\rho}{4}V_{rmc}^2$$

Total power generated by wind turbine

$$P_t = \frac{\rho C_P A V^3}{2} kg.m/s: \ \rho = 1.2929.\frac{273}{T}\frac{P}{760}$$

C. The newly proposed ANN Intelligent control based hybrid electric vehicle charging system.

Structure of the ANN hybrid controller in The suggested ANN in this work uses a hybrid control technique to execute an offline training procedure to obtain appropriate values for the PI controller's main two coefficients, KP and KI. Shown in Figure 6, the ANN contains one input layer, two hidden levels, and one output layer. As shown in Fig. 6, the input layer has two neurons representing the current's error value e(t) and its derivative value de(t), the hidden layers each contain two neurons, and the output layer contains two neurons indicating KP and KI. The q-th hidden layer computes the overall weight value netq and the j-th neuron's output value Zq.

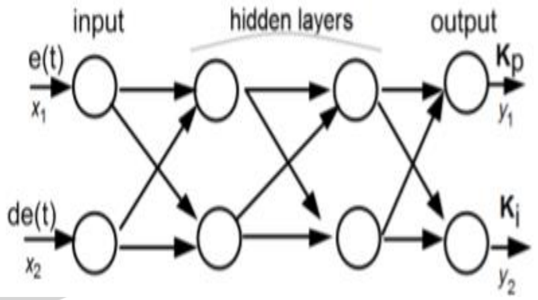

Fig. 6 Detailed structure of the ANN with four layers

$$net_q = \sum v_{qj} x_j \qquad (17)$$

$$z_q = a_h(net_q) = a_h(\sum v_{qj} x_j) \qquad (18)$$

Where vqj denotes the weight increase applied to the jth neuron and is the operating function of the hidden layer. The output layer's total weight value for the i-th neuron is then determined, where wiq is the weight increase of the i-th neuron. Finally, we define the two coefficients KP and KI as follows: where a0(.) is the operating function of the output layer.

$$net_i = \sum w_{iq} z_q = \sum [w_{iq}.a_h(net_q)] \qquad (19)$$

$$K_P = a_0(net_1) = a_0(\sum w_{1q} z_q) = a_0(\sum [w_{1q}.a_h(net_q)]) \qquad (20)$$

$$K_I = a_0(net_2) = a_0(\sum w_{2q} z_q) = a_0(\sum [w_{2q}.a_h(net_q)]) \qquad (21)$$

Where the operating functions of the hidden and output layers are bipolar sigmoid and linear, respectively:

 DOI : 10.35291/2454-9150.2022.0363

ISSN : 2454-9150 Vol-08, Issue-03, June 2022

$$a_h(f) = 1/(1+e^{-f}) \quad (22)$$

$$a_0(f) = f \quad (23)$$

If the number of hidden layers is increased, the ANN may become more adaptive. Two hidden layers, such as the simplest structure for implementation in simulation, may be used to evaluate the proposed ANN algorithm in this research. The training period increases as the number of hidden layers increases, which might result in a perceptible delay in producing the control signal at the output layer. As a result, we'll look at optimising the amount of hidden layers and the time delay in the future. The BP method comprises two primary processes in conveying information between layers, as depicted in Figs. 6: To begin, the input value x(k) is sent forward in order to generate the output value y. (k). The difference between the reference value d(k) in the data set and the output value y(k) is then communicated back to the preceding layer, which adjusts the weight gains vqj correspondingly. Sx(k),d(k) is the data set utilized in the offline training procedure, and the objective of this training is to minimize the error E(k+1). Generally, the offline training approach for ANNs is done out utilizing a large number of data sets to get the desired result.

$$E(k+1) = E(k) + 0.5\sum[d_i(k) - y_i(k)] \to \min \quad (24)$$

V. RESULTS AND DISCUSSION

The simulation results are used to demonstrate the CS's performance.

A. Simulation Results

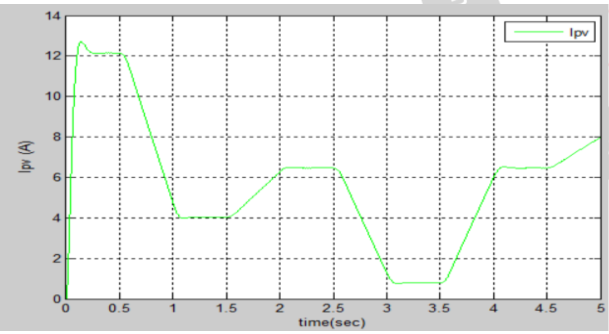

(a)

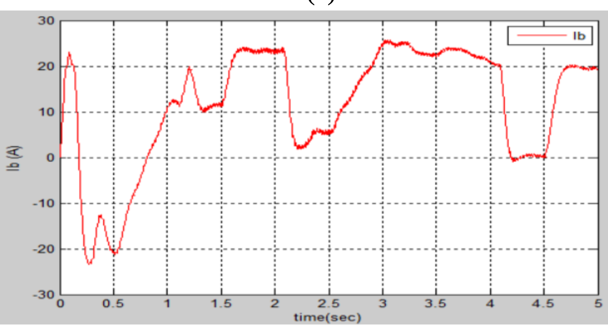

(b)

Fig. 7 (a-b)Simulation results showing the battery performance Wind off Solar present

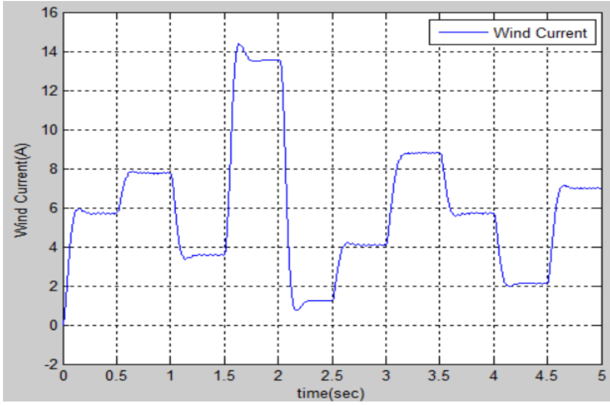

(a)

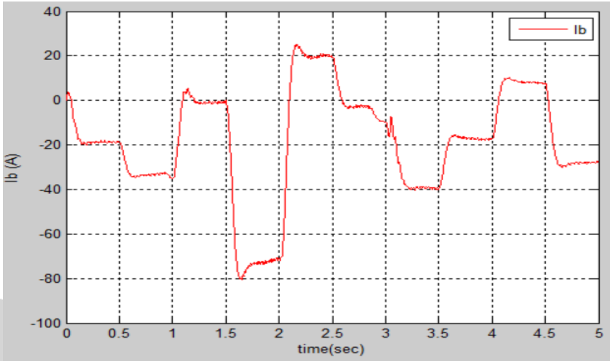

(b)

Fig. 8 (a-b)Simulation results showing the battery performance Solar off and Wind present

The uninterruptible functioning of the CS is shown by simulation results in Figures 7 and 8. The CS is initially in islanded mode, with wind and PV array electricity being used to charge the EVs linked to the PCC. The excess production is kept in the energy storage because the PV array generation exceeds the EV charging needs. The sun irradiation drops from 1000 W/m2 to 300 W/m2, while the wind speed drops from 12 m/s to 7.2 m/s in 0.5s. As a result of this drop in wind and photovoltaic array output, the storage battery begins to discharge in order to maintain uninterruptible charging.

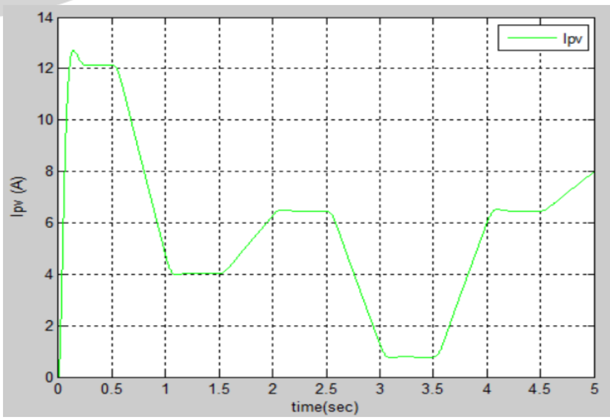

Fig. 9 Simulation results showing the battery performance Solar present

DOI : 10.35291/2454-9150.2022.0363

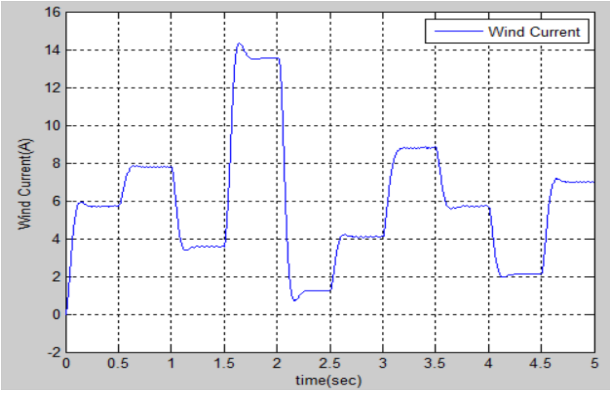

Fig. 10 Simulation results showing the battery performance Wind present

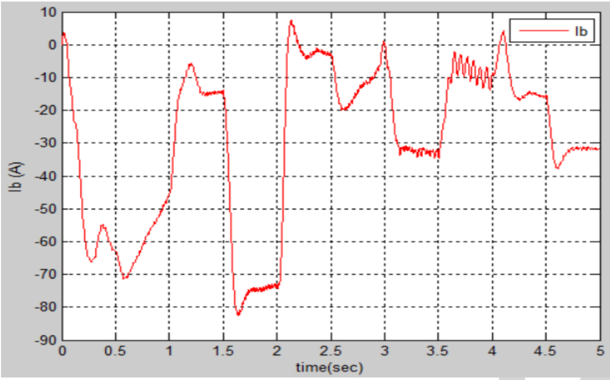

Fig. 11 Simulation results showing the battery performance Battery current

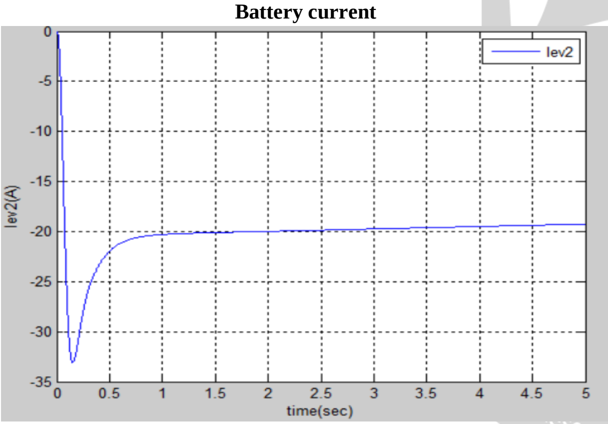

Fig. 12 Simulation results showing the battery performance electric vehicle current

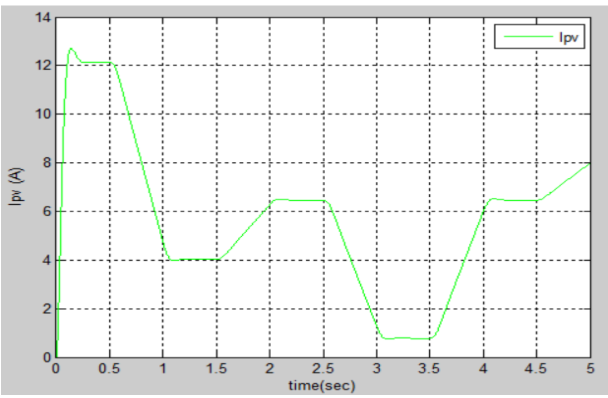

(a)

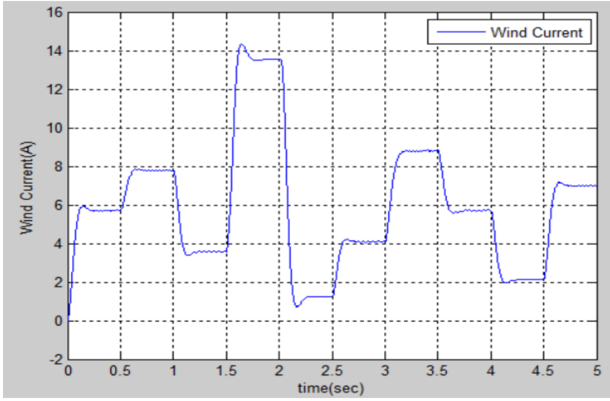

(b)

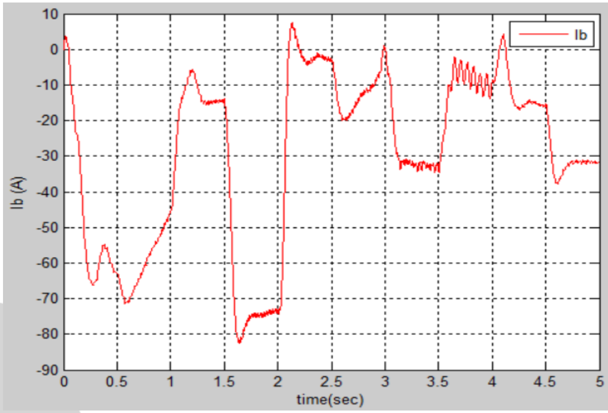

(c)

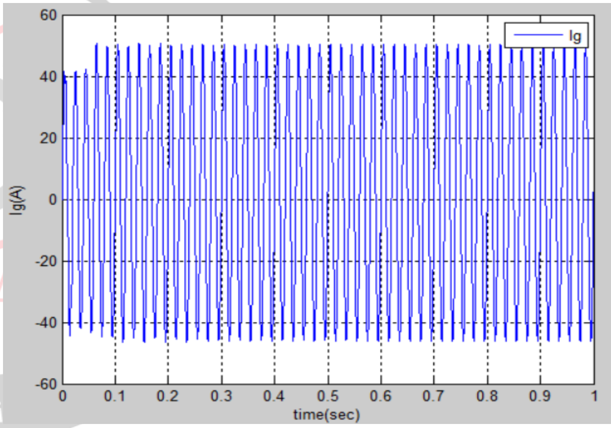

(d)

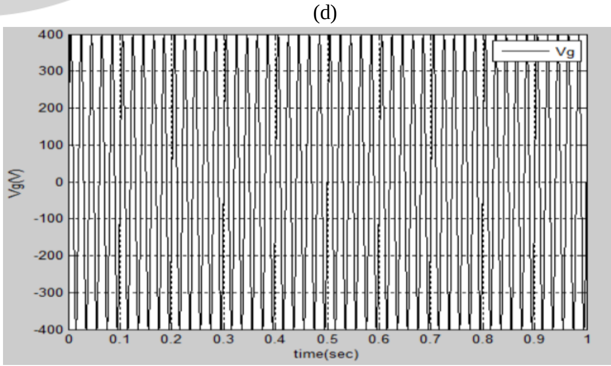

(e)

 DOI : 10.35291/2454-9150.2022.0363

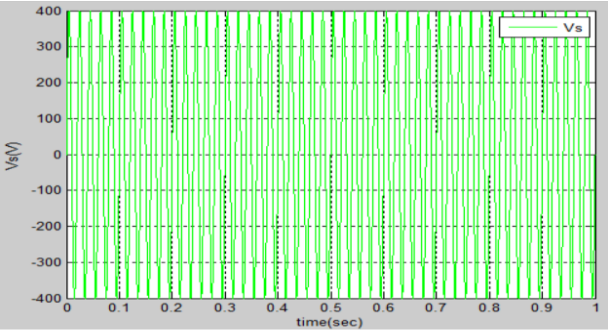

(f)

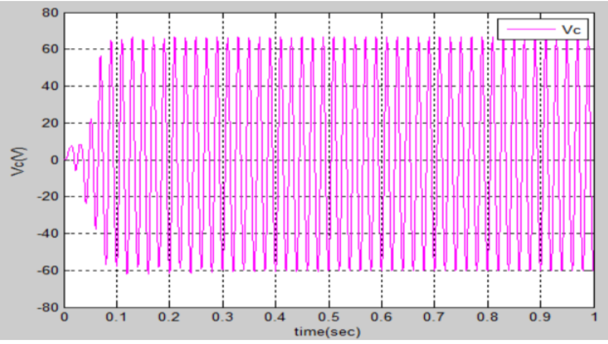

(g)

Fig. 13 Simulation results showing the different modes of operation

The storage battery drains after 2 seconds, when the wind power and PV array power are both zero. After that, as long as the SOC > SOCmin, the storage battery fully enables charging. After the battery has been fully discharged, the controller synchronises the CS and connects it to the grid. The CS began pulling electricity from the grid at 3.5 seconds. Due to the absence of grid and storage battery power at this point, CS is provided by the DG set, as seen in Fig. 9. As seen in Fig. 10, the charging station automatically switches modes based on generation and demand.

VI. CONCLUSION

This paper presents an ANN-based intelligent controller to solve data loss and delay amongst entities in an electric vehicle charging system. An ANN Intelligent control system based on Wind-Solar PV-BES and DEGS System set was created for EV charging. The results reveal that a single VSC can run the CS in many modes (island, grid, and DG set). The suggested intelligent controller performs data integrity checks and adjustments at the input of FLC utilising real-time node voltage data, data predicted by ANN, and historical node voltage trend. Its performance as an independent generator with outstanding voltage quality was proven. In DG set or grid connected mode, the ANN-based control algorithm was able to keep the power exchange with the grid at UPF or the DG set's optimum loading. Islanded, grid and DG set linked, and automatic mode switching have increased the possibility of PV array MPP functioning, DG set optimum loading, and charging reliability. The performance of the conventional FLC and the proposed intelligent controller is compared. With a voltage and current THD of less than 5%, the charging station's IEEE compliance demonstrates its efficiency. Inferring from the foregoing, this charging station can efficiently utilise numerous energy sources while delivering reliable and cost-effective charging to EVs.

REFERENCES

[1] Wang, R., Wang, P. and Xiao, G., 'Two-stage Mechanism for Massive Electric Vehicle Charging Involving Renewable Energy', IEEE Trans. on Vehicular Technology, Vol. PP, no. 99, accepted for publication, Jan. 2016.

[2] Lopes, J. Soares, F. and Almeida, P., 'Integration of Electric Vehicles in the Electric Power System', Proceedings of the IEEE, Vol. 99 , no1, pp. 168-183, Jan. 2011.

[3] Chenrui, J., Sheng, X and Prasanta, G.: Optimized Electric Vehicle Charging With Intermittent Renewable Energy Sources', IEEE Journal of Selected Topics in Signal Processing, 2007, Vol. 8, No. 6, pp. 1063–1072

[4] Jhala, K., Natarajan, B., Erickson, L. et al: "Coordinated electric vehicle charging solutions using renewable energy sources", in Proc. IEEE, Symposium on Computational Intelligence Applications in Smart Grid, Orlando, Florida, USA, Dec. 2014, pp. 1–6

[5] S. Shao, M. Pipattanasomporn, and S. Rahman, "Grid integration of electric vehicles and demand response with customer choice," IEEE Trans. Smart Grid, vol. 3, no. 1, pp. 543–550, Mar. 2012.

[6] H. Khayyam, H. Ranjbarzadeh, and V. Marano, "Intelligent control of vehicle to grid power," J. Power Sources, vol. 201, pp. 1–9, 2012.

[7] International Energy Agency-Global EV Outlook 2018-Towards cross-modal electrification. [Online] Available: https://webstore.iea.org /download/ direct/1045?fileName=Global_EV_Outlook_2018.pdf

[8] International Energy Agency- Renewables 2O18 - Analysis and Forecasts to 2O23 [Online]. Available: https://webstore.iea.org/ download/summary/2312?fileName=English-Renewables-2018ES.pdf.

[9] J. Ugirumurera and Z. J. Haas, "Optimal Capacity Sizing for Completely Green Charging Systems for Electric Vehicles," IEEE Trans. Transportat. Electrificat.vol. 3, no. 3, pp. 565-577, Sept. 2017.

[10] G. R. Chandra Mouli, J. Schijffelen, M. van den Heuvel, M. Kardolus and P. Bauer, "A 10 kW Solar-Powered Bidirectional EV Charger Compatible With Chademo and COMBO," IEEE Trans, Power Electron., vol. 34, no. 2, pp. 1082-1098, Feb. 2019.

[11] V. Monteiro, J. G. Pinto and J. L. Afonso, "Experimental Validation of a Three-Port Integrated Topology to Interface Electric Vehicles and Renewables With the Electrical Grid," IEEE Trans. Ind. Informat., vol. 14, no. 6, pp. 2364-2374, June 2018.

 DOI : 10.35291/2454-9150.2022.0363

[12] S. A. Singh, G. Carli, N. A. Azeez and S. S. Williamson, "Modeling, Design, Control, and Implementation of a Modified Z-Source Integrated PV/Grid/EV DC Charger/Inverter," IEEE Trans. Ind. Electron., vol. 65, no. 6, pp. 5213-5220, June 2018.

[13] K. Chaudhari, A. Ukil, K. N. Kumar, U. Manandhar and S. K. Kollimalla, "Hybrid Optimization for Economic Deployment of ESS in PV-Integrated EV Charging Stations," IEEE Trans. Ind. Informat., vol. 14, no. 1, pp. 106-116, Jan. 2018.

[14] F. Kineavy and M. Duffy, "Modelling and design of electric vehicle charging systems that include on-site renewable energy sources," in IEEE 5th Int. Symp. Power Electron. For Distributed Gene. Syst. (PEDG), Galway, 2014, pp. 1-8.

[15] Y. Zhang, P. You and L. Cai, "Optimal Charging Scheduling by Pricing for EV Charging Station With Dual Charging Modes," IEEE Trans. Intelligent Transportat. Syst., vol. 20, no. 9, pp. 3386-3396, Sept. 2019.

[16] Y. Yang, Q. Jia, G. Deconinck, X. Guan, Z. Qiu and Z. Hu, "Distributed Coordination of EV Charging With Renewable Energy in a Microgrid of Buildings," IEEE Trans. Smart Grid, vol. 9, no. 6, pp. 6253-6264, Nov. 2018.

[17] N. K. Kandasamy, K. Kandasamy and K. J. Tseng, "Loss-of-life investigation of EV batteries used as smart energy storage for commercial building-based solar photovoltaic systems," IET Electrical Systems in Transportation, vol. 7, no. 3, pp. 223-229, 9 2017.

[18] A. Tavakoli, M. Negnevitsky, D. T. Nguyen and K. M. Muttaqi, "Energy Exchange Between Electric Vehicle Load and Wind Generating Utilities," IEEE Trans. Power Sys., vol. 31, no. 2, pp. 1248-1258, 2016.

[19] Y. Shan, J. Hu, K. W. Chan, Q. Fu and J. M. Guerrero, "Model Predictive Control of Bidirectional DC-DC Converters and AC/DC Interlinking Converters - A New Control Method for PV-Wind-Battery Microgrids," IEEE Trans. Sustain. Energy, Early Access.

[20] F. Hafiz, A. R. de Queiroz and I. Husain, "Coordinated Control of PEV and PV-based Storages in Residential System under Generation and Load Uncertainties," IEEE Trans. Ind. Applica., Early Access.

[21] R. W. Wies, R. A. Johnson, A. N. Agrawal and T. J. Chubb, "Simulink model for economic analysis and environmental impacts of a PV with diesel-battery system for remote villages," IEEE Trans. Power Systems, vol. 20, no. 2, pp. 692-700, May 2005.

[22] R. R. Chilipi, N. Al Sayari, A. R. Beig and K. Al Hosani, "A Multitasking Control Algorithm for Grid-Connected Inverters in Distributed Generation Applications Using Adaptive Noise Cancellation Filters," IEEE Trans. Energy Conversion, vol. 31, no. 2, pp. 714-727, June 2016.

AUTHORS PROFILE

K. Ravi Kiran is an Under Graduate student studying IV B.Tech Electrical and Electronics Engineering from Kallam Haranadhareddy Institute of Engineering & Technology, Guntur, A.P, India. His research interests include Power System Operation and Electrical Machines.

K.Srinivasa Rao is an Under Graduate student studying IV B.Tech Electrical and Electronics Engineering from Kallam Haranadhareddy Institute of Engineering & Technology, Guntur,A.P, India. His research interests include Power System Operation and Electrical Machines.

Ch.Ranga Raghava Reddy is an Under Graduate student studying IV B.Tech Electrical and Electronics Engineering from Kallam Haranadhareddy Institute of Engineering & Technology, Guntur, A.P, India. His research interests include Power system operation and Electrical Machines.

V.Ramani is an Under Graduate student studying IV B.Tech Electrical and Electronics Engineering from Kallam Haranadhareddy Institute of Engineering & Technology, Guntur, A.P, India. Her research interests include Power System Operation and Electrical machines.

Mr. K Nagaraju received his B. Tech degree In Electrical and Electronics Engineering from Acharya Nagarjuna University, Guntur, India. in 2008 and M. Tech from NIT Calicut, Kerala, India in 2011. he is having 08 years Of teaching and research experience. He is currently Assistant Professor in the Engineering, Kallam Haranadhareddy Institute of Technology, Guntur, India. His Research interests are in the areas of Control systems and Power System Operation and control.

 DOI : 10.35291/2454-9150.2022.0363